Tissue Eng Regen Med (2018) 15(4):503–510
https://doi.org/10.1007/s13770-018-0142-x

Online ISSN 2212-5469
Print ISSN 1738-2696

ORIGINAL ARTICLE

Wicking Property of Graft Material Enhanced Bone Regeneration in the Ovariectomized Rat Model

Seunghyun Kim[1] · Taeho Ahn[1] · Myung-Ho Han[2] · Chunsik Bae[1] · Daniel S. Oh[3]

Received: 26 May 2018 / Revised: 18 June 2018 / Accepted: 3 July 2018 / Published online: 13 July 2018

Abstract

BACKGROUND: Recruitment and homing cells into graft materials from host tissue is crucial for bone regeneration.
METHODS: Highly porous, multi-level structural, hydroxyapatite bone void filler (HA-BVF) have been investigated to restore critical size bone defects. The aim was to investigate a feasibility of bone regeneration of synthetic HA-BVF compared to commercial xenograft (Bio-Oss). HA-BVF of 0.7 mm in average diameter was prepared via template coating method. Groups of animals (n = 6) were divided into two with normal (Sham) or induced osteoporotic conditions (Ovx). Subsequently, subdivided into three treated with HA-BVF as an experiment or Bio-Oss as a positive control or no treatment as a negative control (defect). The new bone formation was analyzed by micro-CT and histology.
RESULTS: At 4 weeks post-surgery, new bone formation was initiated from all groups. At 8 weeks post-surgery, new bone formation in the HA-BVF groups was greater than Bio-Oss groups. Extraordinarily greater bone regeneration within the Ovx-HA group than Sham–Bio-Oss or Ovx–Bio-Oss group ($p < 0.05$).
CONCLUSION: This study suggests that the immediate wicking property of HA-BVF from host tissue activates a natural healing cascade without the addition of exogeneous factors or progenitor cells. HA-BVF may be an effective alternative for repairing bone defects under both normal and osteoporotic bone conditions.

Keywords Bone regeneration · Hydroxyapatite · Osteoporosis · Bone void filler

1 Introduction

The ultimate goal of hard tissue engineering with grafted materials is their incorporation with host bone, repopulation with endogenous cells, and reconstitution of gas and body fluid exchanges to restore normal bone function. Many leading investigators have demonstrated remarkable outcomes in bone regeneration using graft materials with pre-loaded cells and/or large amounts of signaling molecules, requiring extensive laboratory techniques and excessive costs [1–6]. However, the shortage of biogenic microenvironments within most graft materials has hindered the potential for clinical applications of bone tissue engineering [7, 8]. In these regards, encouraging bone regeneration using resembled natural microenvironment, recruitment and homing endogenous cells into graft

✉ Chunsik Bae
csbae210@chonnam.ac.kr

✉ Daniel S. Oh
danielsunho@gmail.com

[1] College of Veterinary Medicine, Chonnam National University, 77 Yongbong-ro, Gwangju 61186, Republic of Korea

[2] Department of Chemical Engineering, Kyungil University, 50 Gamasil-gil, Gyeongsan 38428, Republic of Korea

[3] Carroll Laboratory for Orthopedic Surgery, Columbia University, 650 West 168th Street, New York, NY 10032, USA

materials, has been spotlighted in bone tissue engineering research. While the past decade, researchers have explored a vast number of techniques to mimic bone characteristics such as, pore size, porosity, interconnectivity, tortuosity, and permeability in synthetic bone grafts. These factors collectively play a vital role in cell migration, proliferation, differentiation, nutrient flow and cell communication, all of which are crucial for proper bone healing [9–14] There remains little consensus concerning optimal pore sizes for bone ingrowth [15], with suggestions ranging from mean pore sizes of 100 um to 500 um diameters [7]. More recently, the presence of microporosity (> 10 μm) has been shown to enhance bone repair [16, 17] possibly by improving fluid flow and promoting neovascularization.

Osteoporosis is one of the most prevalent systemic skeletal disorders in the developed countries. Despite of this prevalence, less attention has been made to the study of osteoporotic bone regeneration utilize synthetic bone grafts than fracture prevention and the development of therapeutics for the enhancement of bone density and bone mass [18–21]. Moreover, many of the previous studies for bone regeneration process utilizing induced osteoporotic animal models were performed in subcritical size defects [22–24]. Despite the proven capability of the established bone regeneration models, the utilization of critical size defects can be considered more foreseeable approach for the validation of translational feasibility of output the intrinsic regenerative potential of the grafted materials. Therefore, in this work, we aim to assess the ability of a hydroxyapatite-based multi-level structural bone void filler (HA-BVF) to support osteoblast-like cell proliferation and differentiation results in bone regeneration compared to a commercial bovine bone graft (Bio-Oss). Bio-Oss was selected for the comparison study because Bio-Oss is one of the most popular grafting materials in the clinics [25]. Along with the hypothesis that harmonized micro-structure with speedy wicking property of the HA-BVF would better support cell infiltration and repopulation. Bone regeneration feasibility in the ovariectomize-induced osteoporotic rat model compared to the control animals (Sham rats) were performed. The calvarial critical size, 8 mm in diameter, defect model was used, and surgical defects were implanted with Bio-Oss as a positive control or innovative HA-BVF as an experimental of proven biocompatibility and bone regeneration capability.

2 Materials and methods

2.1 Overall study design

Animals were randomly divided into two groups: ovariectomy (Ovx) and Sham (control surgery). Following 8 weeks, all animals were submitted to a surgical bicortical craniotomy (8 mm circular critical size defect), which was filled with a synthetic bone graft (HA-BVF) or commercial xenograft (Bio-Oss). Animals were euthanized at 4 and 8 weeks following graft implantation, and the orthotopic bone regeneration was evaluated by radiographic, microtomographic, histological, and histomorphometric techniques.

2.2 Fabrication of multi-level structural bone void filler

A nano-sized hydroxyapatite (HA) powder was synthesized by reacted calcium hydroxide and phosphoric acid. To obtain granulated HA-BVF ranging 0.5–1.0 mm in diameter, a porous and fully interconnected cancellous-bone-like scaffold was fabricated followed by a previous publication [26]. Briefly, 2.0 wt% poly(vinyl alcohol) (Sigma-Aldrich) and 0.5 wt% carboxymethyl cellulose (Sigma-Aldrich) were used as binders. As an anionic dispersant, 2.0 wt% ammonium polyacrylate (R.T. Vanderbilt Company, USA) was added and 0.5 wt% glycerin was added as a drying agent (Sigma-Aldrich). After obtained the powder/solution ratio 1.7 of HA mixture, polyurethane sponge template was coated and dried, then heat treated at 1230 °C for 3 h. The trabecular bone-like scaffold was granulated using mortar and pestle with sieve into the experiment size.

2.3 Characterization of HA-BVF

The three-level structures and sizes of HA-BVF were examined using stereo microscope, scanning electron microscope (SEM: JEOL 5700, Tokyo, Japan), and micro computed tomography (micro-CT: SKYSCAN 1272, Kontich, Belgium). Elemental analysis after heat treatment was assessed using X-ray diffraction. The upper-micro and micro pore size range was directly determined by measuring the diameter of pores on SEM images compared with scale bar and magnification.

2.4 Animals

All animal procedures were approved by the Institutional Animal Care and Use Committee of Chonnam National University (CNU IACUC-YB-R-2014-37) and the animals were cared for in accordance with the Guidelines for Animal Experiments of Chonnam National University. All surgical procedures were conducted under general anesthesia, and postoperative analgesic care was ensured with tramadol. All efforts were made to minimize animal suffering and distress. Briefly, 72 female Sprague–Dawley rats (11 weeks old, 248.9 ± 11.11 g; Samtaco, Osan, Korea) were used for each group (n = 6). Animals were randomly divided into Ovx or Sham operation and further divided into three groups depending on defect treatment after Sham

or Ovx operation; negative control (Defect: unfilled defect), positive control (filled with Bio-Oss®, Geistlich, Wolhusen, Switzerland), and experimental (filled with HA-BVF). The bone regeneration process was assessed at 4 and 8 weeks following the establishment of bone defects.

2.5 Ovx and Sham operation

The animals were fasted for 12 h before anesthesia. Preoperatively, the rats were weighed and received atropine (0.1 mg/kg; Jeil Pharmaceutical, Daegu, Korea) and enrofloxacine (2.5 mg/kg; Bayerkorea, Seoul, Korea) subcutaneously. Anesthesia was induced and maintained with mixture of xylazine (10 mg/kg; Bayerkorea, Seoul, Korea) and ketamine (40 mg/kg; Yuhan Co., Seoul, Korea) by intraperitoneal injection. The operation sites were shaved and sterilized with povidone-iodine and alcohol. Under sterile conditions, ovaries were approached by two separate flank incisions through the skin and muscle. The ovary was gently pulled, and a hemostat was placed at the uterine horns. A ligature was placed with 4-0 silk below the hemostat. The ovary was cut off and the uterus was returned to the abdomen. The abdominal muscle layer was sutured with absorbable 4-0 suture (Surgisorb, Samyang Co., Seoul, Korea). The skin was closed with non-absorbable 3-0 suture (Silk, Ailee Co., Busan, Korea). The same procedure except placement of the ligatures and ovary removal was performed to all animals of the Sham group. After surgery, rats were injected with 3 ml of warm normal saline subcutaneously.

2.6 Calvarial critical size defect surgery

Following 8 weeks from Ovx or Sham operation, general anesthesia was performed with the same protocol of first surgery. The skin of rat head was shaved and disinfected. Skin incision was performed, and exposed periosteum was incised L-shaped and separated from the skull bone with blunt scraping. A circular critical size bone defect was created using a trepan bur (8 mm in diameter). Defects were left unfilled or filled with Bio-Oss or HA-BVF. The periosteum was sutured using 4-0 absorbable suture. The skin was closed with 3-0 non-absorbable suture. Each animal received a subcutaneous injection of tramadol (10 mg/kg) at 12, 24, and 36 h after surgery for continued postoperative analgesia.

2.7 Assessment of the bone regeneration

At 4 and 8 weeks following implantation, harvested calvarias of both Sham and Ovx animals were freshly evaluated by gross examination and subsequently stored in 10% buffered formalin for radiographic, microtomographic, and histological analysis (n = 6). Radiographic imaging protocol for fixed calvaria samples were conducted with digital dental X-ray and intraoral radiology unit (Elytis, Trophy, MARNE LA VALLEE CEDEX 2, Croissy-Beaubourg, France). X-ray scan was performed at 60 kVp, 4 mA, film-focus distance of 20 cm and exposure time of 0.344 s. Micro-CT scan was performed for microtomographic analysis. An X-ray tube voltage of 70 kVp, a current intensity of 220 μA, and an integration time of 500 ms were used. The region of interest was manually selected involving the defect area. Quantification of bone volume was performed using CTAn software (BRUKER, Kontich, Belgium). Three-dimensional images were also obtained for visualization, display, and analysis. Histomorphometric analyses were performed using Bioquant image analysis software (Nashville, TN, USA) which allowed calibrated calculation of the area of tissue sections. Briefly, the total bone area, newly formed bone area, and bone graft area were manually delimited. Subsequently, bone volume per tissue volume (BV/TV) and bone graft volume per tissue volume (BSV/TV) were determined. Fixed calvaria samples were processed for undecalcified histological preparation. Ground sections, 20–30 μm thickness, were generated using an EXAKT Grinding System (EXAKT Technologies, Norderstedt, Germany). Sections were stained with hematoxylin and eosin. The most central portion of each defect, including the section displaying the widest extension, was identified and subjected to histologic and histomorphometric analysis.

2.8 Statistical analysis

All data are reported as mean—standard error of the mean. Significance in histological and micro-CT analysis was determined using a two-way ANOVA and Tukey's test for post hoc evaluation. Significance in new bone formation was determined using a one-way ANOVA and Tukey's test for post hoc evaluation. The significance level was set at $p < 0.05$.

3 Results

3.1 Clinical observation

During the study period, no complications were identified from both the Ovx and Sham surgery. Any significant pathological alterations or the presence of abnormal fluids were not found in any animal.

3.2 Optimal microstructure of BVF

HA-BVF was engineered with three leveled structures consisting of primary upper-micron sized pores

(~ 400 μm) for bone ingrowth, micron sized channels (~ 70 μm) within each granule to induce wicking property, and sub-micron (~ 400 nm) sized holes on its surface to encourage cells to anchor. Owing to micro channels, the granules also provided doubled surface area when compared to others to enlarge cell attachment. In general, higher surface area boosts cell proliferation which results to enhanced bone regeneration. Moreover, roughened surfaces with nano characteristics may induce osteogenic differentiation of cells (Fig. 1) [27–29].

By these combinatorial synergistic, HA-BVF was completely saturated with blood which may have endogenous stromal elements within seconds. Meanwhile, Bio-Oss graft merely filled the bony defect without wicking of blood (Fig. 2).

3.3 Bone regeneration

All animals reported a steady increase in body weight during the study period. At 4 and 8 weeks following craniotomy, Ovx rats weighted significantly more than Sham animals. In order to confirm the 8 mm defects were critical size and thus would not be healed without intervention, empty defects left to heal without implantation, were conducted in both Sham and Ovx animals. The empty defects displayed the growth of a thin fibrous tissue layer with less amount of isolated new bone formation, as observed in the representative radiographic image at 8 weeks of healing following craniotomy (Fig. 3). On the other hand, grafted defects displayed a retention of the granules and new bone formation as shown in the representative images of the 8 weeks healing time.

3.4 Microtomographic and histomorphometric evaluation

After craniotomy and graft implantation, microtomographic analysis was performed (Fig. 4). Since the graft materials have a high density and the high-resolution acquisition (bright white) than newly regenerated bone (light gray) in the defect area reorganization of graft materials could be easy. Even though relatively low amount of new bone formation was identified throughout the period of time, a little higher newly formed bone was depicted in the HA-BVF group either Sham and Ovx model. Through the sagittal view, the newly formed bone was evidenced in light gray throughout and in close contact with the implanted granular material in both Sham and Ovx samples. The transverse view offered details of the bone regeneration process from the vicinity of the defect margin to center. Amazingly, the highest new bone formation was distinguished in Ovx animals with HA-BVF implantation. Accordingly, lots of engulfed HA-BVF by newly formed mineralized tissue (dotted rectangle) and an enhanced newly formed bone within the implanted HA-BVF surface (triangles) was identified. Unexpectedly, far less amount of new bone formation was observed in Sham animals with Bio-Oss with no signs of engulfment and reduced amount of mineralized tissue on its surface (triangles). Based on the gray-scale value, quantitative analysis of the bone volume within the tissue volume (BV/TV) was used to determine the overall bone regeneration. Surprisingly, BV/TV was lower in Sham animals comparing to Ovx animals in the HA-BVF group. Significant differences were attained at 8 weeks' time point (Fig. 4). The bone graft volume per tissue volume (BSV/TV) was also calculated, and no significant differences between experimental groups were found.

3.5 Histological evaluation

Histological sections were analyzed for further investigation of the incorporation and tissue response of graft materials and the bone tissue ingrowth within defects. Overall and representative high-magnification histological samples are shown in Fig. 5. At 4 weeks, a typical new

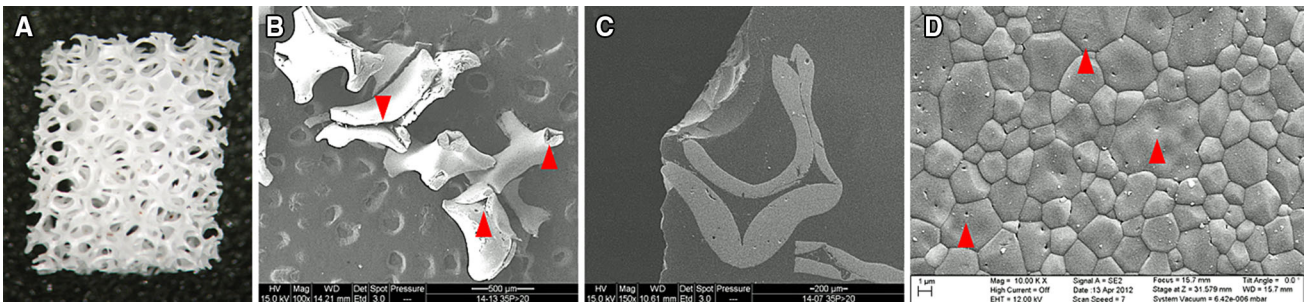

Fig. 1 Digital and scanning electron microscope (SEM) images of biogenic microenvironment scaffold. **A** Overall image of hydroxyapatite-based scaffold. **B** SEM image of granulated HA-BVF with micro-channels (red arrow head). **C** Representative image of micro-channel inside of each graule. **D** Surface image of granule. Clear grain boundaries and nano-pores (red arrow head) were identified. (Color figure online)

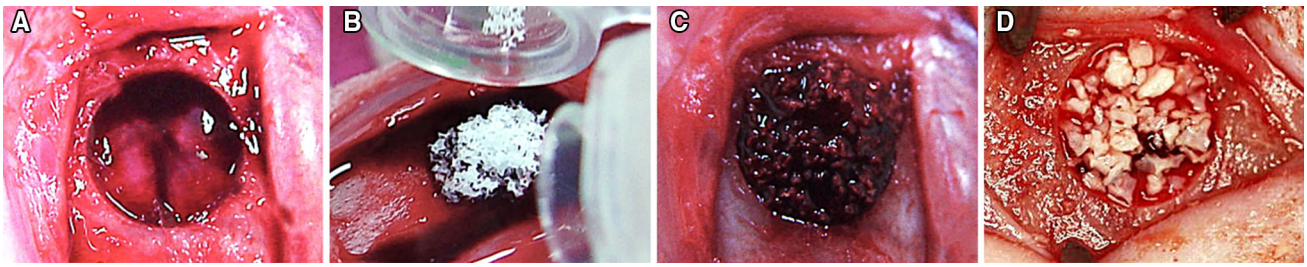

Fig. 2 Surgical procedures and wicking property of granulated HA-BVF. **A** Creation of 8 mm diameter bony defect in calvaria. **B** Placement of granulated HA-BVF into defect. **C** Speedy wicking property of HA-BVF. **D** No sucking property with control Bio-Oss

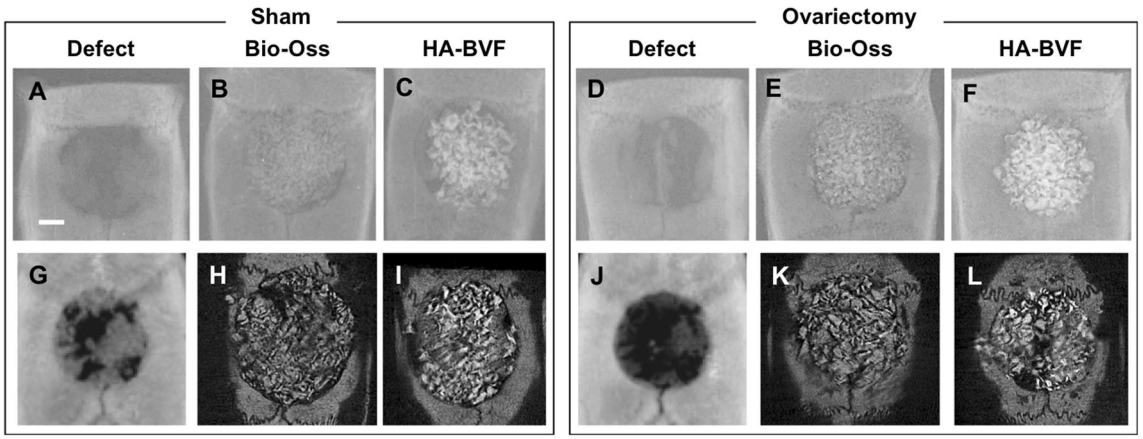

Fig. 3 **A–F** Radiographic (upper row) and **G–L** microtomographic (lower row) evaluation of the bone regeneration (n = 6). Representative radiographic images of calvarial 8 mm diameter critical size defect after 8 weeks of craniotomy. Surgical defects were left unfilled or implanted with Bio-Oss or HA-BVF granules in Sham animals **A, G** defects, **B, H** Bio-Oss, **C, I** HA-BVF, and in Ovx animals **D, J** defects, **E, K** Bio-Oss, **F, L** HA-BVF. Scale bar represents 2 mm

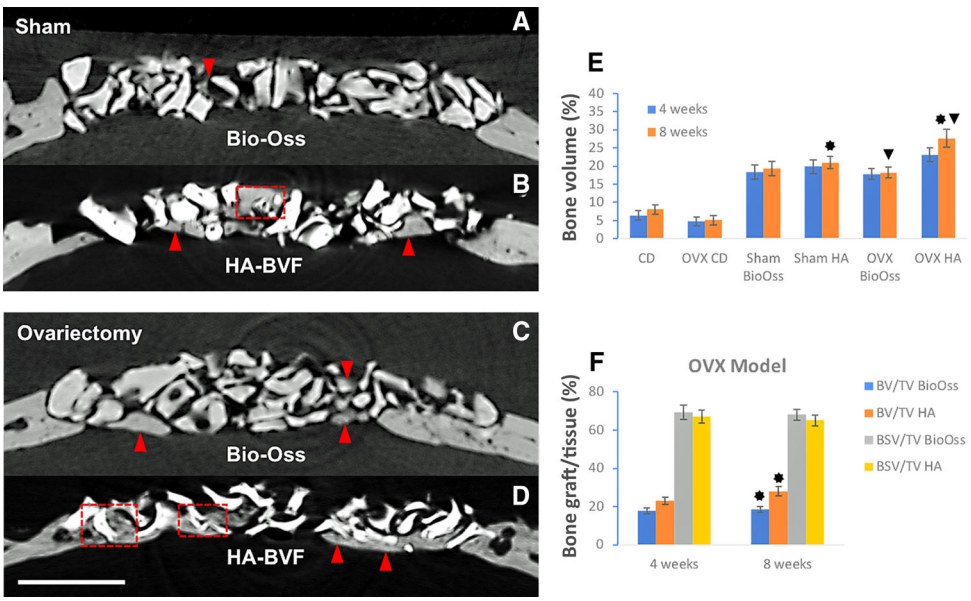

Fig. 4 Representative microtomographic images of calvarial 8 mm critical size defects, implanted with **A** Bio-Oss, **B** HA-BVF granules in Sham animals and **C** Bio-Oss, **D** HA-BVF in Ovx animals to heal for 8 weeks. Scale bar represents 2 mm-left. **E** Percentage of the Bone Volume (BV) attained in Sham and Ovx animals, throughout 8 weeks of healing following craniotomy. Asterisk and arrow head—significantly different from Sham-HA and OVX-BioOss. **F** Percentage of the BSV/TV attained in OVX model for 8 weeks healing

bone ingrowth from the defect margin was initiated toward the center of the defect throughout entire groups. In the Bio-Oss group, the majority of grafted granules were found restrained to the defect region and enveloped by fibrous tissue. In adjacent areas to the defect margin both in Sham and Ovx samples within Bio-Oss group, some granules seem to be partially bordered by a very thin layer of mineralized tissue. Even at 8 weeks, not much progressed

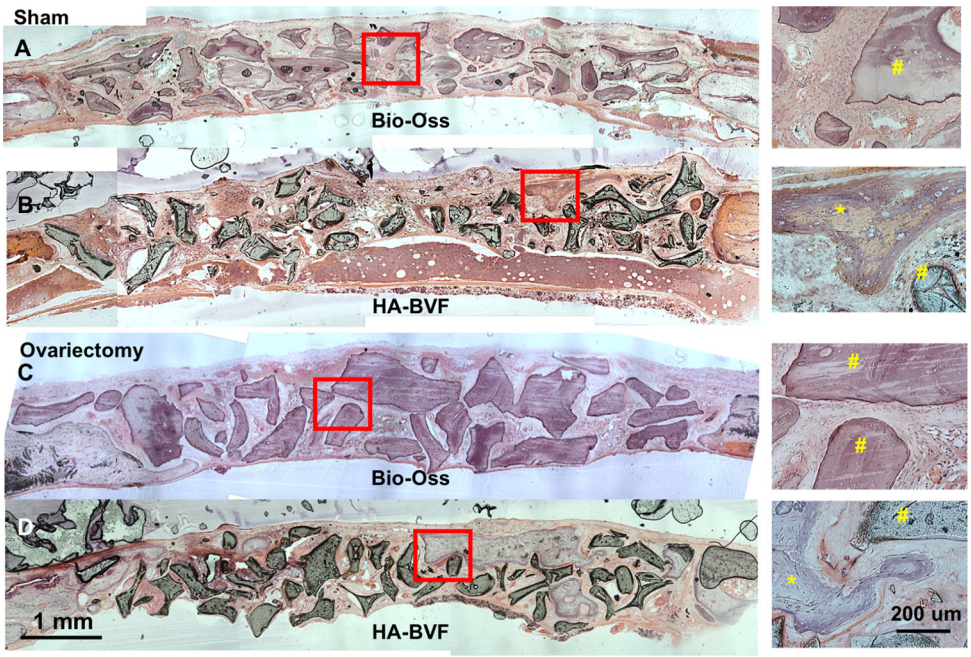

Fig. 5 Histological analysis of bone regeneration of calvarial 8 mm critical size defects (n = 6). Representative undecalcified sections implanted with **A** Bio-Oss, **B** HA-BVF granules in Sham animals and **C** Bio-Oss, **D** HA-BVF in Ovx animals to heal for 8 weeks following craniotomy, stained with hematocylin and eosin. Asterisk marks areas of newly formed mineralized tissue; pound sign marks areas of implanted bone graft. Red squares indicate higher field to right columns

bone ingrowth and new bone formation was identified in both Sham and Oxv with the Bio-Oss implantation. The majority of implanted granules were interspaced by fibrous tissue; nonetheless, some newly formed mineralized tissue could be seen in the granules' border. But the Bio-Oss granules entrapment by the regenerative process was not evidenced. On the other hand, an enhanced bone formation was visualized throughout the defect in both Sham and Ovx animals within the HA-BVF group (Fig. 5). Moreover, the engulfment of HA-BVF granules into the newly formed bone at the margin of the defect as well as center region was clearly evidenced.

4 Discussion

In this study, two study aim was tested. Firstly, is the wicking property of the HA-VBF can be altered bone regeneration than others? Secondly, is the bone regeneration capability of the HA-BVF with speedy wicking property also reproducible under osteoporotic conditions? In completion of these two aims, may the study provide alternative treatment plan for the patients in both normal and osteoporotic circumstances.

Osteoporosis is a metabolic disorder that characterized by an inadequate bone remodeling, thus resulting in decreased bone mass and inducing microarchitectural deterioration of the skeleton. Despite substantial research in the osteoporotic bone alterations, the regeneration process study via bone graft materials is far less reported in this systemically affected circumstance. Moreover, despite the proven capability of the established bone regeneration in subcritical size models, the utilization of critical size defects under osteoporotic bone conditions can be provided wide spectrum in biomaterial medicated bone regeneration. The Ovx rat model is commonly applied in post-menopausal osteoporosis-related research that exhibit loss of bone density, as well as a significant decreased mechanical strength. Hence, the use of critical size defect with induced osteoporosis model consists of an increased regenerative challenge. Accordingly, the proposed study model allowing the evaluation of the intrinsic regenerative potential of the HA-VBF [30, 31].

In both Sham and Ovx animals implanted with Bio-Oss, the bone regeneration process was slowed even after 8 weeks of healing and broadly distributed close to the defect margin. On the other hand, in both Sham and Ovx animals treated with HA-BVF, qualitative data from microtomographic, histological analysis, and histomorphometric data, presented greater bone regeneration than Bio-Oss. A curious finding within HA-BVF groups is that superior bone regeneration was demonstrated in Ovx animals than Sham animals being significant differences attained at 4 and 8 weeks healing. Even HA-BVF was implanted without a requirement for the additional exogenous factors, such as bone morphogenetic protein or a population of progenitor cells. Surprisingly, our data is inconsistent with previous literature reports of bone regeneration in Ovx rat model associated with bone graft materials. The achievement of hard tissue regeneration in critical size defects must rely on the osteoconductive, osteoinductive, or osteogenic capabilities of the grafted

materials. And, in the absence of potent osteoinductive or osteogenic stimuli of grafted materials widely fail to output significant tissue regeneration [32]. In this regard, the saturation of blood with cells and stromal elements from surrounding tissue into grafted materials may be considered as resources of osteoinductive or osteogenic capabilities. Accordingly, as shown in Fig. 2, HA-BVF demonstrated immediate saturation of blood into HA-BVF in surgical site. This speedy saturation may have induced by combinatorial synergistic which is hydrophilic surface property of HA and micro-nano channel structures in the granules. These properties are also agreed with previous results [26, 33]. Hence, we postulate that this phenomenon may accelerate cells migration with stromal elements result in cell homing to enhance bone regeneration. Simultaneously, the importance of characteristics in bone graft materials has been well described. Key features include a range of pore sizes on both the macro and micro scale, interconnectivity of the pores, allowing fluid diffusion and cell migration through the material, and finally a degree of tortuosity. The granulated HA-BVF provides all of these features with 39.7% microporosity, 34.2% macroporosity, 97.6% interconnectivity and permeability similar to that of human bone. On the other hand, the use of a xenograft, which is gifted with only osteoconductive properties due to the shortage of initial cell homing and stromal elements absorption, may establish a slow bone healing process.

Based on the previous literatures, the outcomes of new bone formations were varying among studies. Variances of outcomes of bone regeneration in both Sham and Ovx model in the available literature might be, at least in part, justified by differences in the experimental design include evaluation periods and different characteristics of biomaterials. Consequently, establishing direct comparisons between studies is difficult. However, a selection of used bone graft material, which can provide biogenic microenvironment, is utmost significance. To favoring those with an improved osteoconductive, osteoinductive, and osteogenic performance in order to prospectively improve the bone healing.

Overall, the HA-BVF demonstrated better osseous healing than with commercially available bone graft (Bio-Oss). Furthermore, the greatest bone regeneration was demonstrated in Ovx models treated with HA-BVF at 8 weeks post implantation. Therefore, newly developed hydroxyapatite-based highly porous composed of multi-level structure granulated bone void filler (HA-BVF) demonstrated excellent candidacy for bone regeneration in both normal patients and osteoporotic patients. However, the reason for the paramount bone regeneration phenomenon in Ovx model is unclarified in this study. Thus, further study to clarify this phenomenon is suggested.

Acknowledgements This study was partially supported by Chonnam National University, 2016 and Basic Science Research Program through the National Research Foundation of Korea (NRF) funded by Ministry of Education (2017R1D1A1B03034829).

Compliance with ethical standards

Conflict of interest The authors declare no conflict of interest.

Ethical statement Animal experimental procedures were approved by the Institutional Animal Care and Use Committee of Chonnam National University (CNU IACUC-YB-R-2014-37) and the animals were cared for in accordance with the Guidelines for Animal Experiments of Chonnam National University.

References

1. Petrie Aronin CE, Sadik KW, Lay AL, Rion DB, Tholpady SS, Ogle RC, et al. Comparative effects of scaffold pore size, pore volume, and total void volume on cranial bone healing patterns using microsphere-based scaffolds. J Biomed Mater Res A. 2009;89:632–41.
2. Guzmán R, Nardecchia S, Gutiérrez MC, Ferrer ML, Ramos V, del Monte F, et al. Chitosan scaffolds containing calcium phosphate salts and rhBMP-2: in vitro and in vivo testing for bone tissue regeneration. PLoS One. 2014;9:e87149.
3. Jabbarzadeh E, Starnes T, Khan YM, Jiang T, Wirtel AJ, Deng M, et al. Induction of angiogenesis in tissue-engineered scaffolds designed for bone repair: a combined gene therapy-cell transplantation approach. Proc Natl Acad Sci U S A. 2018;105:11099–104.
4. Cha JK, Lee JS, Kim MS, Choi SH, Cho KS, Jung UW. Sinus augmentation using BMP-2 in a bovine hydroxyapatite/collagen carrier in dogs. J Clin Periodontol. 2014;41:86–93.
5. Zhao J, Zhang Z, Wang S, Sun X, Zhang X, Chen J, et al. Apatite-coated silk fibroin scaffolds to healing mandibular border defects in canines. Bone. 2009;45:517–27.
6. Kim HJ, Kim UJ, Kim HS, Li C, Wada M, Leisk GG, et al. Bone tissue engineering with premineralized silk scaffolds. Bone. 2008;42:1226–34.
7. Karageorgiou V, Kaplan D. Porosity of 3D biomaterial scaffolds and osteogenesis. Biomaterials. 2005;26:5474–91.
8. Vats A, Tolley NS, Polak JM, Gough JE. Scaffolds and biomaterials for tissue engineering: a review of clinical applications. Clin Otolaryngol Allied Sci. 2003;28:165–72.
9. Woodard JR, Hilldore AJ, Lan SK, Park CJ, Morgan AW, Eurell JA, et al. The mechanical properties and osteoconductivity of hydroxyapatite bone scaffolds with multi-scale porosity. Biomaterials. 2007;28:45–54.
10. Zong C, Qian X, Tang Z, Hu Q, Chen J, Gao C, et al. Biocompatibility and bone-repairing effects: comparison between porous poly-lactic-co-glycolic acid and nano-hydroxyapatite/poly(lactic acid) scaffolds. J Biomed Nanotechnol. 2014;10:1091–104.
11. Unger RE, Sartoris A, Peters K, Motta A, Migliaresi C, Kunkel M, et al. Tissue-like self-assembly in cocultures of endothelial cells and osteoblasts and the formation of microcapillary like structures on three-dimensional porous biomaterials. Biomaterials. 2007;28:3965–76.
12. Zhang J, Zhou H, Yang K, Yuan Y, Liu C. RhBMP-2-loaded calcium silicate/calcium phosphate cement scaffold with hierarchically porous structure for enhanced bone tissue regeneration. Biomaterials. 2013;34:9381–92.
13. Hofmann S, Hagenmüller H, Koch AM, Müller R, Vunjak-Novakovic G, Kaplan DL, et al. Control of in vitro tissue-engineered

bone-like structures using human mesenchymal stem cells and porous silk scaffolds. Biomaterials. 2007;28:1152–62.
14. Correia C, Bhumiratana S, Yan LP, Oliveira AL, Gimble JM, Rockwood D, et al. Development of silk-based scaffolds for tissue engineering of bone from human adipose-derived stem cells. Acta Biomater. 2012;8:2483–92.
15. Bohner M, Loosli Y, Baroud G, Lacroix D. Commentary: deciphering the link between architecture and biological response of a bone graft substitute. Acta Biomater. 2011;7:478–84.
16. Hing KA, Annaz B, Saeed S, Revell PA, Buckland T. Microporosity enhances bioactivity of synthetic bone graft substitutes. J Mater Sci Mater Med. 2005;16:467–75.
17. Lan Levengood SK, Polak SJ, Wheeler MB, Maki AJ, Clark SG, Jamison RD, et al. Multiscale osteointegration as a new paradigm for the design of calcium phosphate scaffolds for bone regeneration. Biomaterials. 2010;31:3552–63.
18. Poole KE, Treece GM, Ridgway GR, Mayhew PM, Borggrefe J, Gee AH. Targeted regeneration of bone in the osteoporotic human femur. PLoS One. 2011;6:e16190.
19. Leppänen OV, Sievänen H, Jokihaara J, Pajamäki I, Kannus P, Järvinen TL. Pathogenesis of age-related osteoporosis: impaired mechano-responsiveness of bone is not the culprit. PLoS One. 2008;3:e2540.
20. Khosla S, Westendorf JJ, Oursler MJ. Building bone to reverse osteoporosis and repair fractures. J Clin Invest. 2008;118:421–8.
21. Dominguez LJ, Scalisi R, Barbagallo M. Therapeutic options in osteoporosis. Acta Biomed. 2010;81 Suppl 1:55–65.
22. Teófilo JM, Brentegani LG, Lamano-Carvalho TL. Bone healing in osteoporotic female rats following intra-alveolar grafting of bioactive glass. Arch Oral Biol. 2004;49:755–62.
23. Okazaki A, Koshino T, Saito T, Takagi T. Osseous tissue reaction around hydroxyapatite block implanted into proximal metaphysis of tibia of rat with collagen-induced arthritis. Biomaterials. 2000;21:483–7.
24. Tami AE, Leitner MM, Baucke MG, Mueller TL, van Lenthe GH, Müller R, et al. Hydroxyapatite particles maintain peri-implant bone mantle during osseointegration in osteoporotic bone. Bone. 2009;45:1117–24.
25. Xuan F, Lee CU, Son JS, Jeong SM, Choi BH. A comparative study of the regenerative effect of sinus bone grafting with platelet-rich fibrin-mixed Bio-Oss® and commercial fibrin-mixed Bio-Oss®: an experimental study. J Craniomaxillofac Surg. 2014;42:e47–50.
26. Oh DS, Koch A, Eisig S, Kim SG, Kim YH, Kim DG, et al. Distinctive capillary action by micro-channels in bone-like templates can enhance recruitment of cells for restoration of large bony defect. J Vis Exp. 2015. https://doi.org/10.3791/52947.
27. Starý V, Douděrová M, Bačáková L. Influence of surface roughness of carbon materials on human osteoblast-like cell growth. J Biomed Mater Res A. 2014;102:1868–79.
28. Zhou H, Wu X, Wei J, Lu X, Zhang S, Shi J, et al. Stimulated osteoblastic proliferation by mesoporous silica xerogel with high specific surface area. J Mater Sci Mater Med. 2011;22:731–9.
29. Ito H, Sasaki H, Saito K, Honma S, Yajima Y, Yoshinari M. Response of osteoblast-like cells to zirconia with different surface topography. Dent Mater J. 2013;32:122–9.
30. Hollinger JO, Kleinschmidt JC. The critical size defect as an experimental model to test bone repair materials. J Craniofac Surg. 1990;1:60–8.
31. Gomes PS, Fernandes MH. Rodent models in bone-related research: the relevance of calvarial defects in the assessment of bone regeneration strategies. Lab Anim. 2011;45:14–24.
32. Bosch C, Melsen B, Vargervik K. Importance of the critical size bone defect in testing bone-regenerating materials. J Craniofac Surg. 1998;9:310–6.
33. Oh DS, Kim YH, Ganbat D, Han MH, Lim P, Back JH, et al. Bone marrow absorption and retention properties of engineered scaffolds with micro-channels and nano-pores for tissue engineering: a proof of concept. Ceram Int. 2013;39:8401–10.